Post-Source Decay in the Analysis of Polystyrene by Matrix-Assisted Laser Desorption/Ionization Time-of-Flight Mass Spectrometry

Robert J. Goldschmidt, Stephanie J. Wetzel, William R. Blair, and Charles M. Guttman

Polymers Division, National Institute of Standards and Technology, Gaithersburg, Maryland, USA

Various secondary series are observed in matrix-assisted laser desorption/ionization (MALDI) time-of-flight mass spectra of polystyrene. The number and positions of the series depend on the choice of matrix and added cation. For a given treatment, series observed in linear mode are not necessarily observed in reflectron mode, and vice versa. Post-source decay analysis was used to determine that the secondary series arise at least in part from formation and decay of adducts of polystyrene with matrix species. There is some treatment-to-treatment variation, but adduct formation and decay were observed for all tested treatments. The multiplicity of secondary series makes it unclear whether post-source decay occurs for the main series (polystyrene + cation)$^+$ ions under the conditions normally used for polystyrene analysis. Such ions do undergo post-source decay at laser fluences greater than normally used. Although only polystyrene was investigated in this work, other polymers may also produce adduct and decay series in MALDI analysis. Their presence can mask the presence of minor components in a sample, but at least as observed here, do not have a strong influence on molecular mass determinations. (J Am Soc Mass Spectrom 2000, 11, 1095–1106) © 2000 American Society for Mass Spectrometry

Both quantitative and qualitative information can be obtained from the matrix-assisted laser desorption/ionization (MALDI) analysis of polymers [1–5]. The accuracy of quantitative information, such as the number average (M_N) and mass average (M_W) molecular masses, depends on reproduction of the true molecular mass distribution (MWD) in the mass spectrum, or at least on obtaining a representation that differs from the true MWD in a predictable way. Although various discrimination effects can be problematic [6–11], MALDI is considered capable of providing reliable quantitative information for polymers of narrow MWD [12–16]. Understanding of the causes of discrimination is not complete, but it is clear that problems worsen with increasing polydispersity of samples [14, 15].

Qualitative information includes determination of repeat unit and end group masses [12, 17–19] and compositional information for copolymers [20–23]. The amount of qualitative information obtainable from a MALDI mass spectrum depends mainly on how well the peaks, due to the various oligomeric species in a sample, are resolved. Besides instrument-related limitations to resolution, the appearance of extra series of peaks due to attachment of more than one type of cation or to the formation of adducts between polymer and matrix can hinder the recovery of qualitative information [24].

Another potential source of difficulty in extracting qualitative information is fragmentation of ions. MALDI is considered a "soft" ionization method, in that there is usually little or no prompt (i.e., occurring virtually at the time of ion formation) fragmentation of analyte ions. In general, this is beneficial for polymer analysis, because fragmentation of the ions formed from a polymer sample could lead to exceedingly complex mass spectra. On the other hand, fragmentation may in some cases be desirable, because potentially it can provide valuable structural information. There have been several recent reports of the application of collision-induced dissociation (CID) to polymer samples [19, 25–31].

Although prompt fragmentation of analyte ions in MALDI is not common, it is well known that in the analysis of biological molecules by MALDI, metastable decay can occur [32–42]. For MALDI performed on time-of-flight (TOF) mass analyzers, as is most commonly the case, the ability to analyze fragment ions

Address reprint requests to Dr. Robert J. Goldschmidt, National Institute of Standards and Technology, 100 Bureau Drive Stop 8541, Gaithersburg, MD 20899-8541, E-mail: robert.goldschmidt@nist.gov

1044-0305/00/$20.00
PII S1044-0305(00)00177-X

Received May 25, 2000
Revised July 17, 2000
Accepted July 18, 2000

depends upon the mode of operation. Especially for metastable ions, the appearance of fragment peaks depends upon the use of linear or reflectron modes and delayed or continuous extraction. It is also useful to distinguish between in-source decay and decay occurring in the field-free drift region. On linear TOF instruments, promptly formed fragments appear at their true mass-to-charge ratio (m/z) in a mass spectrum that has been calibrated to give the true m/z values of intact ions [43]. Metastable fragmentation occurring during acceleration will result in fragment ions of a given mass being spread over a wide range of arrival times. However, with delayed extraction, decay occurring before application of the accelerating voltage will again result in fragment ions that can be assigned based on the normal, intact ion calibration of the linear mass spectrum [41, 42].

Fragment ions produced in the drift region are more difficult to assign. In linear TOF instruments, such post-source decay (PSD) ions will have similar arrival times at the detector as the corresponding parent ion. In reflectron TOF instruments, the reflector field will cause a separation in time of arrival of such fragments and the corresponding parent ion. The fragment ions can therefore be distinguished from the parents, but a mass spectrum calibrated for intact ions will not give the true m/z values of the fragment ions. In addition, at a given reflector voltage setting, only a limited mass range of PSD ions will be focused at the detector [34–36, 38]. The reflector voltage must be stepped to bring other ranges into focus. Calibration of PSD ions can be accomplished from knowledge of the relevant instrument voltages and distances, along with the parent ion mass, or by comparison to the fragment peaks observed for a parent with known PSD behavior [35, 36, 38].

When a sample contains a mixture of analytes, PSD analysis may be difficult, because it may not be clear which ion is the source of PSD fragments. Pulsed ion deflectors, which allow only parent ions of a chosen m/z window to enter the reflector, are thus commonly used [35, 36, 38]. Any PSD fragments that appear in the mass spectrum must then emanate from ions included in the accepted window. This is certainly relevant to polymer samples, especially those that may give rise to several series of ions.

To date, PSD has had only limited application to polymer samples in MALDI [28]. Although this may be simply due in part to the few attempts to apply the technique, it may also reflect a lower tendency of synthetic polymers to undergo PSD in comparison to biological molecules. Sources of internal energy that may lead to PSD include interactions with matrix species during desorption and collisions in the desorbed plume and with residual gas molecules during flight through the instrument [33]. For samples run under similar conditions, the energies acquired by synthetic polymer molecules and biological molecules from these sources are likely to be similar. Another significant cause of PSD may be energy acquired during proton or cation attachment [39]. Polymer molecules are likely to acquire less internal energy from metal cation attachment than biomolecules from proton attachment [44]. Also, in some cases polymer ions may require a relatively high level of internal energy to cause bond breaking.

In this work, we investigate the source of various secondary series observed in MALDI mass spectra of polystyrene (PS). We originally observed unexpected secondary series in the reflectron mode mass spectrum of a PS sample that was supposed to have oligomers with a single set of end groups, *t*-butyl and hydrogen [45]. As suggested above, such series could arise due to the presence of PS oligomers having end groups other than the expected ones, to ionization of PS by other than attachment of the expected cation (silver or copper), or by formation of adducts between PS oligomers and the matrix or the salt employed. In reflectron mode mass spectra, another possible source of secondary series is PSD. In the course of our investigation, a total of six different matrix-cation treatments were used, and linear mode, reflectron mode, and PSD mass spectra were examined. It became apparent that adduct formation and decay were common in the MALDI analysis of PS, at least for the treatments investigated. Although some adducts and decay products could be identified with confidence, others aspects remain uncertain. There are several factors that hinder a more complete understanding, not the least of which is the distributive nature of polymer samples.

Experimental

Mass spectra were acquired on a Bruker Reflex II TOF mass spectrometer equipped with dual microchannel plate detectors for both linear and reflectron modes and with a 3-ns pulsewidth nitrogen laser (337 nm) [46]. A pulsed ion deflector allows selection of a mass window for PSD analysis. Delayed extraction was used during the acquisition of all mass spectra. The matrices trans-retinoic acid (RA, FW 300.45), trans-3-indoleacrylic acid (IAA, FW 187.20), and dithranol (FW 226.23) and the salts silver trifluoroacetate (AgTFA, FW 220.88) and copper trifluoroacetate [Cu(II)TFA, FW 289.57] were acquired from Aldrich [46] and used as received. Solutions were prepared using tetrahydrofuron (THF) (Mallinckrodt, Paris, KY) [46] solvent. THF was reagent grade and stabilized with butylated hydroxytoluene (BHT), 0.025%. Two PS samples were used, PS7900 and PS3900, where the numbers indicate the nominal molecular weights assigned by the manufacturer. Both samples were obtained from Polymer Source (Dorval, Quebec, Canada) [46]. The PS7900 sample was prepared to order by anionic polymerization using a *t*-butyllithium initiator. The PS3900 sample also has butyl and hydrogen end groups. Typically, matrix-to-analyte molar ratios were 1500:1 for PS3900 and 3000:1 for PS7900, and matrix-to-cation molar ratios were 200:1. Though no systematic investigation of sample preparation vari-

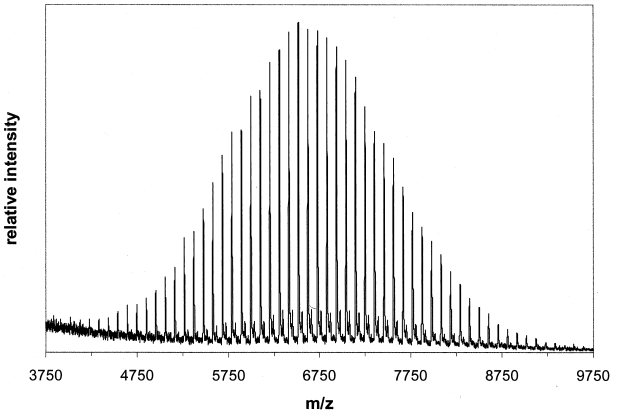

Figure 1. Reflectron mode MALDI mass spectrum of PS7900 taken using the RA/AgTFA treatment. Secondary series peaks appear at about +40 *m/z* with respect to the main series, $(PS + Ag)^+$ peaks.

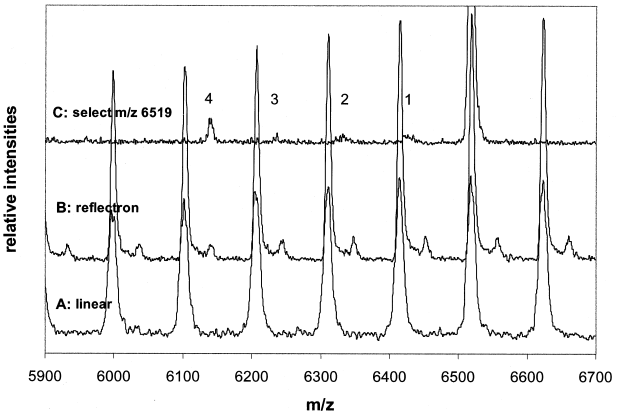

Figure 2. Partial MALDI mass spectra of PS7900 obtained using the RA/AgTFA treatment and (**A**) linear mode, (**B**) reflectron mode, and (**C**) using pulsed ion deflector to select *m/z* 6519 ± 50 u. Peaks marked 1 through 4 are PSD fragments emanating from parents in the selection window. Spectrum **C** is calibrated for the parent ion, not the fragments.

ables was performed, matrix-to-analyte ratios between 500:1 and 10,000:1 and matrix-to-cation ratios between 50:1 and 300:1 were tried, and these gave at least qualitatively similar results to those achieved with the typical ratios. A few experiments were performed using chloroform as a solvent and also with silver nitrate as a cation source. These gave results not noticeably different from those reported, and so they are not discussed separately. PSD fragment mass assignment was performed using the Bruker XTOF software, based on calibration of fragments from the 18–39 clip of the peptide ACTH.

Results and Discussion

Experiments Using PS7900

Figure 1 contains a reflectron mode mass spectrum of the PS7900 sample obtained using RA matrix and AgTFA. The main series of peaks is due to ions having the expected nominal *m/z* values $[58 + (104.15)_n + 108]^+$, where 108 u is the average mass of silver and 58 u is the combined mass of the *t*-butyl and hydrogen end groups. A second series of peaks appears at +40 *m/z* relative to the main series. Each of the other five treatments also produces one or more secondary series in its reflectron mode mass spectra; however, the positions of the secondary peaks in relation to the expected main series peaks are different in each case. For example, for the dithranol/AgTFA treatment secondary series appear at +20 and +60 *m/z*, and for the RA/Cu(II)TFA treatment a secondary series appears at +35 *m/z*, with respect to the main series. The presence in the sample of PS oligomers with different than the expected end groups is unlikely to account for these series, especially because infrared (IR) and proton nuclear magnetic resonance (NMR) spectra did not reveal the presence of any end groups besides the expected *t*-butyl and hydrogen [45].

In the linear mode mass spectra obtained using the RA/AgTFA treatment (Figure 2A) there are no obvious secondary series, suggesting that the reflectron mode secondary peaks (Figure 2B) are due to PSD of main series ions. This interpretation is supported when a main series ion is selected for PSD analysis, as in Figure 2C. Four fragment peaks emanate from the selected mass window. The spectrum is calibrated for the parent ion, and comparison to Figure 2B indicates that it is the fragment marked 4 in Figure 2C that gives rise to the secondary series. The three higher mass fragments are not resolved in Figure 2B, but contribute to the shoulder between the peaks of the main series and largest fragment series. When the PSD spectrum is calibrated for the fragment ions, the peak positions shift to lower mass and appear to match up with main series ions. The fragment mass assignments are consistent with main series ion masses to within 3 u or better. Thus, before considering evidence from the other treatments, these PSD results suggest that the selected main series ion undergoes losses of multiples of 104 u, i.e., elimination of styrene repeat units. Thus, for example, fragment peak 1 is consistent with loss of one styrene unit, fragment 2 is consistent with loss of two styrene units, and so on.

Three of the other treatments give results similar to those of the RA/AgTFA treatment, i.e., no secondary series are apparent in the linear mode spectra, and when a mass window containing a main series ion is selected, PSD products are obtained that are apparently due to losses of styrene units from the selected ion. Figure 3 contains PSD spectra for the four treatments that follow this pattern [A: RA/AgTFA, B:IAA/AgTFA, C: dithranol/AgTFA, and D: dithranol/Cu(II)TFA]. Although the same losses appear to occur for each treatment (the offset of the decay peaks in Figure 3D is due to the attachment of copper rather than silver), the intensity pattern is different in each case. This accounts for the differences among the treatments in the posi-

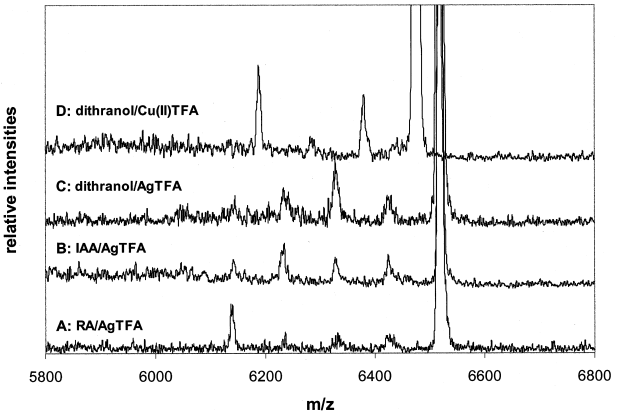

Figure 3. Partial MALDI mass spectra of PS7900 obtained using the pulsed ion deflector to select the $(PS_{n=61} + M)^+$ ion and the treatments (**A**) RA/AgTFA, (**B**) IAA/AgTFA, (**C**) dithranol/AgTFA, and (**D**) dithranol/Cu(II)TFA. Peaks in **D** are offset due to the attachment of copper rather than silver. All spectra are calibrated for the parent ions.

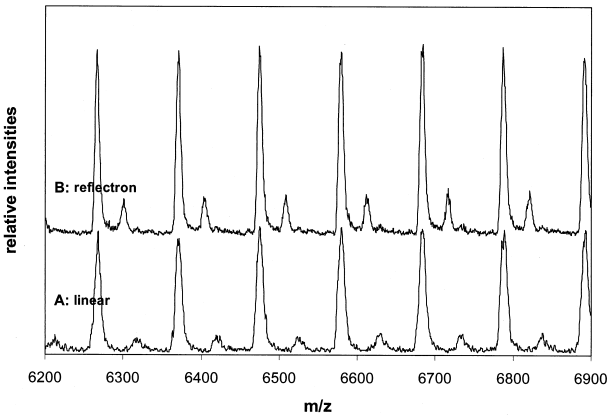

Figure 4. Partial (**A**) linear mode and (**B**) reflectron mode MALDI mass spectra of PS7900 obtained using the RA/Cu(II)TFA treatment. Mass selection experiments indicate that the largest of the secondary series in **B** is due to PSD of the secondary series ions in **A**. A smaller secondary series in **B** matches the series in **A**.

tions of the secondary series that are visible in the reflectron mode mass spectra.

If the secondary series are due to PSD of main series ions, it remains to explain why each treatment produces a different fragment intensity pattern. This would require influence of both matrix and cation on the decay process. Such influence could conceivably come about due to effects on parent ion internal energy or due to some structural influence on the fragmentation pathway. In the former case it would be implied that the reactions leading to elimination of different numbers of styrene repeat units are competitive, rather than consecutive, and that there are significant thermodynamic or kinetic differences among the competing reactions. The latter case could perhaps come about due to differences in parent ion conformation. Conformational differences are a possibility for silver cationized versus copper cationized parents, but the nature of a matrix influence is not obvious.

The results obtained for the other two treatments [RA/Cu(II)TFA and IAA/(Cu(II)TFA] raise more doubts about whether the secondary series are due to PSD of main series ions. In these cases secondary series are observed in the linear mode spectra as well as in the reflectron mode spectra. Mass spectra for the RA/Cu(II)TFA treatment are shown in Figure 4. The linear mode secondary series (Figure 4A) is offset from the largest of the reflectron mode secondary series (Figure 4B), though there is a smaller series in the reflectron mode that does appear to match up with it. Mass selection experiments show that the largest reflectron mode secondary series is due to decay of the linear mode secondary series ions and not of the main series ions. Similar results are found for the IAA/Cu(II)TFA treatment. The linear mode secondary series could perhaps be due to in-source fragmentation of main series ions. That would indicate that in these cases main series ions undergo consecutive losses to yield the PSD products observed in reflectron mode. It would be expected in the case of in-source fragmentation that daughter ions would be correctly mass identified using the same calibration as used for the parent ions [41, 42]. However, we could not make any probable assignment of the linear mode secondary series as PS fragments for either of the treatments. The linear mode secondary series could alternatively be due to adduct formation. However, it was only after analysis of the mass spectra of a second PS sample, as will be discussed next, that we were able to identify likely adducts.

Experiments Using PS3900

Secondary series observed for the PS3900 sample are similar to those observed for the PS7900 sample; however, additional series are visible. Improved peak definition at the lower mass range is likely to account for the appearance of most, if not all, of the additional series. Of particular note is that for the PS3900 sample, secondary series are apparent in the linear mode spectra of not only the RA/Cu(II)TFA and IAA/Cu(II)TFA treatments, but also the dithranol/Cu(II)TFA and IAA/AgTFA treatments. This enabled the recognition that for each of these treatments the same relation holds between the peak positions of the most prominent linear mode secondary series and the main series. The secondary series peaks are separated from the main series peaks by the mass of a matrix molecule plus a metal atom. Linear mode spectra for the PS3900 sample are shown in Figure 5A, B, obtained using the IAA/AgTFA and IAA/Cu(II)TFA treatments, respectively. In Figure 5A, the secondary series peak at *m/z* 4106 differs in mass from the $n = 35$ main series ion at *m/z* 3811 by 295 u, which nominally matches the mass of (Ma + Ag), where Ma = matrix. Each of the labeled secondary peaks in Figure 5A is likewise nominally 295 u higher in mass than a corresponding main series peak. In Figure

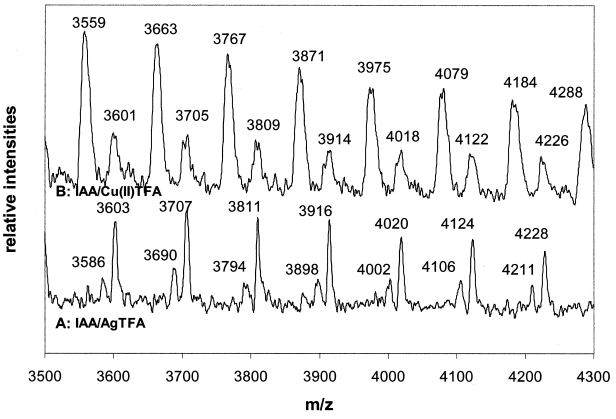

Figure 5. Partial linear mode MALDI mass spectra of PS3900 obtained using the treatments (**A**) IAA/AgTFA and (**B**) IAA/Cu(II)TFA. The marked secondary peaks in **A** are each 295 u higher in mass than a main series $(PS + Ag)^+$ ion. The difference corresponds to the mass of (IAA + Ag). Similarly, in **B** the mass difference between the marked series corresponds to the mass of (IAA + Cu).

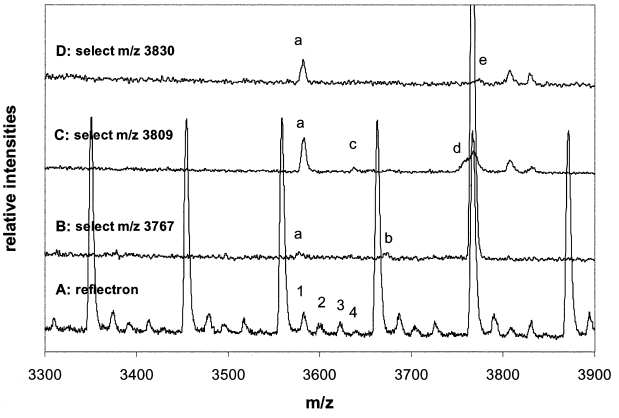

Figure 6. Partial (**A**) reflectron mode and (**B**, **C**, **D**) PSD mode MALDI mass spectra of PS3900 obtained using the IAA/Cu(II)TFA treatment. The PSD spectra are calibrated for parent ions. In **B**, selecting the $(PS_{n=35} + Cu)^+$ ion at *m/z* 3767 (with mass window ±40 u) gives two small fragment peaks, marked a and b. In **C** the $(PS_{n=35} + MaSalt + Cu)^+$ ion at *m/z* 3809 is selected (±40 u). Two fragment peaks, marked a and c, are observed, along with the broad peak marked d. In **D** the ion assigned as $(PS_{n=35} + 2Cu)^+$ at *m/z* 3830 is selected (±40 u). A fragment marked a and another possible fragment, e, are observed. Assignment of the marked peaks is discussed in the text.

5B the secondary peaks are nominally 251 u greater in mass than a corresponding main series ion, a difference that matches the mass of (Ma + Cu). In both treatments, the ions of the most prominent linear mode secondary series are therefore assigned as adducts.

The adducts are most likely of the form $(PS + MaSalt + M)^+$, where MaSalt = (Ma − H + M) and M = Ag or Cu. Adducts of this type have previously been reported for polybutadiene and polyisoprene [24], but to our knowledge, adduct formation in MALDI analysis of PS has not been previously reported. As discussed below, adducts of the form $(PS + Ma + 2M)^+$, which differ in mass by only 1 u from $(PS + MaSalt + M)^+$, may also be formed. Note that in both spectra in Figure 5 there are possibly additional linear mode secondary series, though they are not well defined. They will be discussed further below.

It has been pointed out above for PS7900 that for the IAA/Cu(II)TFA and RA/Cu(II)TFA treatments, PSD products emanate from linear mode secondary series ions and not from the main series ions. Having determined that these linear mode series are due to adduct formation, it is reasonable to suspect that losses of MaSalt, Ma, or M from the adducts could produce reflectron mode secondary series. PSD experiments using the PS3900 sample confirm such decay but reveal a more complicated picture than is apparent with the PS7900 sample. Assignments of the reflectron mode secondary series observed for the IAA/Cu(II)TFA treatment of PS3900 are relatively straightforward, and so these are considered first.

A reflectron mode spectrum of the PS3900 sample obtained using the IAA/Cu(II)TFA treatment is shown in Figure 6A, and PSD spectra are shown in Figure 6B–D. In Figure 6A, four secondary series are visible. Considering a single group of four peaks as marked in the figure, the middle two are assigned as adducts. Peak 2 is assigned as the $(PS + MaSalt + Cu)^+$ adduct. Mass calibration favors that assignment over $(PS + Ma + 2Cu)^+$. Peak 3 is assigned as an adduct of form $(PS + 2Cu)^+$. This is supported by the appearance of a similar series for all three of the Cu(II)TFA treatments. Peaks 1 and 4 are due to adduct decay.

When the main series ion at *m/z* 3767, $(PS_{n=35} + Cu)^+$, is selected (Figure 6B), two small fragments, marked a and b, are observed. Mass calibration of the fragments gives assignments that are consistent with losses of two and one styrene units, respectively, from the main series ion. Fragment peak a apparently makes some contribution to peak 1, but it is not the main contribution, as suggested by comparing Figure 6B to Figure 6C, D. Fragment peak B does not give rise to a visible peak in Figure 6A.

When the $(PS_{n=33} + MaSalt + Cu)^+$ ion at *m/z* 3809 is selected (Figure 6C), the $(PS_{n=35} + 2Cu)^+$ ion at *m/z* 3830 is included in the mass selection window. The converse is also true (Figure 6D). Either of these ions could be the source of the PSD products that appear in Figure 6C, D. The following assignments are made assuming that each, in turn, is the parent.

Two PSD product ions, marked a and c, are apparent in Figure 6C. Fragment mass calibration indicates that a is due to a loss of MaSalt to give $(PS_{n=33} + Cu)^+$. This ion clearly matches up with peak 1. Note that the relative intensity of the $(PS + MaSalt + Cu)^+$ peak is significantly reduced upon changing from linear mode (Figure 5B) to reflectron mode (Figure 6A). Thus most of the ions that leave the source as $(PS + MaSalt + Cu)^+$ adducts decay before reaching the reflector. Decay peak c in Figure 6C, which matches peak 4 in Figure 6A, is consistent with loss of a matrix molecule from the

selected ion. This suggests that in addition to $(PS_{n=33} + MaSalt + Cu)^+$, there may also be formation of $(PS_{n=33} + Ma + 2Cu)^+$ adducts. Note that this decay product does not appear in Figure 6D. The broad peak marked d is probably due to $(PS_{n=35} + Cu)^+$ ions at the edge of the mass window.

In Figure 6D the ion assigned as $(PS_{n=35} + 2Cu)^+$ is selected. Fragment a fits an assignment of loss of Cu plus loss of two styrene units from the selected ion. Although not seen in Figure 6D, a small peak that can be assigned as loss of Cu plus loss of one styrene unit is also sometimes observed upon selection of $(PS_{n=35} + 2Cu)^+$. The small peak marked e fits loss of Cu from the selected ion, though it is possibly due merely to $(PS_{n=35} + Cu)^+$ ions at the edge of the mass window.

The foregoing discussion indicates that decay of three different parent ions may contribute to peak 1 of Figure 6A, with each decay process producing a product ion with formula $(PS_{n=33} + Cu)^+$. As noted, loss of two styrene units from $(PS_{n=35} + 2Cu)^+$ apparently makes only a small contribution. The centroid of the resulting peak is also offset slightly from that of peak 1. The peak position of a PSD ion depends upon the parent ion mass, so some offset is expected. To determine the relative importance of the contributions from decay of $(PS_{n=33} + MaSalt + Cu)^+$ and $(PS_{n=35} + 2Cu)^+$ requires closer examination. Loss of MaSalt from the former ion is intuitively a more probable loss than loss of Cu plus loss of two styrene units from the latter; still, experimental confirmation is desirable. An obvious approach is to achieve isolation of these ions by narrowing the mass selection window. There is, however, a practical limit to this strategy. The fundamental problem is the limited mass selectivity achievable at the position in the first drift region where ion selection occurs [43]. A related problem is that the edges of the ion selector voltage pulses cause reduced peak intensities and distortions in peak positions. In the case under consideration, narrowing the mass window is helpful and confirms that the main contribution to peak 1 is loss of MaSalt from $(PS_{n=33} + MaSalt + Cu)^+$. Total isolation of the two peaks cannot be achieved without a severe reduction in peak intensities, however, so a small contribution from loss of Cu plus loss of 208 u from $(PS_{n=35} + 2Cu)^+$ is not ruled out.

For the RA/Cu(II)TFA treatment, the reflectron mode secondary series and PSD assignments are quite similar to those discussed for the IAA/Cu(II)TFA treatment. A series assigned as $(PS + MaSalt + Cu)^+$ is observed, and the most prominent secondary series can be assigned as loss of MaSalt from those ions. A series assigned as loss of Ma from $(PS + Ma + 2Cu)^+$ is also found. Small peaks assigned as loss of styrene units from $(PS + Cu)^+$ are observed. A series assigned as $(PS + 2Cu)^+$ is found, with possible decay products as discussed above. For the remaining treatments, the assignments are not all as straightforward. Two factors make some assignments more difficult: the presence of additional secondary series and smaller mass separation between series. Nevertheless, loss of MaSalt from the ions of the $(PS + MaSalt + M)^+$ adduct series can account for a reflectron mode secondary series for each of the treatments, including the two for which no definite linear mode $(PS + MaSalt + M)^+$ series is observed. For five of the six treatments this decay produces the dominant secondary series. The exception is the dithranol/AgTFA treatment, discussed more fully below, for which there are multiple reflectron mode secondary series, but no dominant one.

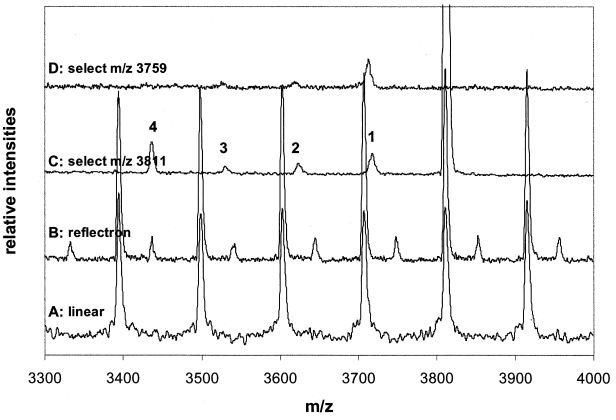

Figure 7. Partial (**A**) linear mode, (**B**) reflectron mode, and (**C, D**) PSD mode MALDI mass spectra of PS3900 obtained using the RA/AgTFA treatment. The PSD spectra are calibrated for parent ions. In **C**, selecting the $(PS_{n=35} + Cu)^+$ ion at *m/z* 3811 with mass window ±50 u gives four fragment peaks, marked 1, 2, 3, and 4. In **D**, an apparently barren region of the spectrum is selected (*m/z* 3759 with mass window ± 30 u). Three fragment peaks are obtained, roughly matching peaks 1, 2, and 3 in **C**.

RAA/AgTFA Treatment

Interpretation of the results from the RA/AgTFA treatment is complicated by the small mass separation between the $(PS + MaSalt + M)^+$ and $(PS + M)^+$ series. The former is shifted by only −9 u compared to the latter, which is the smallest separation between the two series for any of the treatments. If mass spectra from the RA/AgTFA treatment are considered apart from the results of the other treatments, there is little reason to suspect the formation of $(PS + MaSalt + Ag)^+$ adducts. In the linear mode spectrum of Figure 7A, the $(PS + MaSalt + Ag)^+$ peaks are not clearly discernible, though they may be presumed to contribute to the low mass shoulders of the $(PS + Ag)^+$ peaks. The low intensity features visible just to the left of some of the $(PS + Ag)^+$ peaks in the reflectron mode spectrum (Figure 7B) are perhaps due to $(PS + MaSalt + Ag)^+$ adducts that have not decayed, but these features are too small and irregular to confidently be called a series.

Assuming that $(PS + MaSalt + Ag)^+$ adducts are formed with this treatment, when the $(PS_{n=35} + Ag)^+$ ion is selected as in Figure 7C, the $(PS_{n=31} + MaSalt + Ag)^+$ adduct is also passed and vice versa. When it is assumed that $(PS_{n=35} + Ag)^+$ is the source of the decay

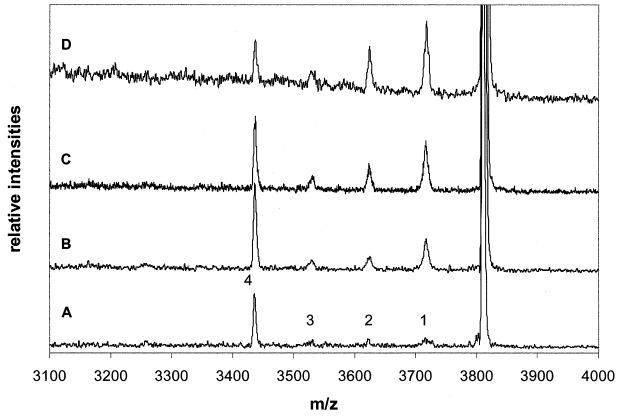

Figure 8. Partial PSD mode MALDI mass spectra of PS3900 obtained using the RA/AgTFA treatment. In each of the spectra **A**, **B**, **C**, and **D** the $(PS_{n=35} + Ag)^+$ ion at *m/z* 3811 is selected with a mass window of ±50 u. The relative intensity of fragment peak 4, relative to those of fragment peaks 1, 2, and 3, changes as laser fluence increases from bottom (near threshold) to top.

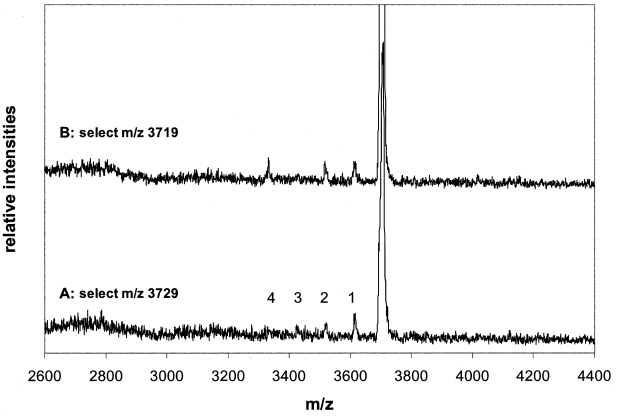

Figure 9. Partial PSD mode MALDI mass spectra of PS3900 obtained using the RA/AgTFA treatment. The spectra are calibrated for parent ions. In **A** the selection window is set to *m/z* 3729 ± 30 u and little or no signal is observed at the position of peak 4. In **B** the selection window is set to *m/z* 3719 ± 30 u and peak 4 is observed.

products, their mass assignments are consistent with loss of styrene units, as was discussed above for the PS7900 sample. When it is assumed that $(PS_{n=31} + MaSalt + Ag)^+$ decays, the assignment of fragment peak 4 is consistent with a loss of MaSalt. There does not appear to be a loss of Ma peak, though it could contribute to a broadening of fragment peak 3. There are no probable losses from $(PS_{n=31} + MaSalt + Ag)^+$ that fit peaks 1 or 2. Although peaks 1, 2, and 3 thus appear to come from decay of $(PS_{n=35} + Ag)^+$, the assignment of peak 4 requires further consideration.

Figure 8 shows the influence of increasing the laser intensity on the fragments observed when $(PS_{n=35} + Ag)^+$ is selected. Peak 4 is by far the most intense fragment peak at laser intensities near the threshold for observing $(PS + Ag)^+$ ions (Figure 8A). As the laser intensity is raised successively in Figure 8B, C, and then to above twice the threshold level in Figure 8D, the intensities of peaks 1, 2, and 3 relative to that peak 4 increase. Note that the intensity ratios among peaks 1, 2, and 3 are near constant. This suggests that these three peaks are related in some way that distinguishes them from peak 4. We should point out that for all treatments secondary peaks were visible over the entire range of laser fluences tested, though, as suggested by Figure 8, there is generally some effect of laser fluence on the intensity patterns.

Another distinction between peak 4 and peaks 1, 2, and 3 can be observed by selecting to either side of a $(PS + Ag)^+$ peak. For example, in Figure 9A, B the selection window is centered not on the $(PS_{n=34} + Ag)^+$ peak at *m/z* 3707, but at masses that include that peak in the lower mass half of the windows. In Figure 9A the window is centered on *m/z* 3729 and fragment peaks 1, 2, and 3 are observed. There is little or no signal for fragment peak 4. In Figure 9B the selection window is moved to center on *m/z* 3719, and all four fragment peaks are observed. Thus it appears that fragment 4 comes from a parent lower in mass than do fragments 1, 2, and 3. If fragments 1, 2, and 3 do come from $(PS_{n=34} + Ag)^+$, then adduct decay is likely to produce peak 4, and as the parent, $(PS_{n=30} + MaSalt + Ag)^+$ has to be considered the most probable candidate. Such an interpretation of peak 4 is supported by its consistency with the results of the other five treatments. As noted above, this interpretation is also attractive because it provides a reasonable explanation as to why, at normally used laser fluences, peak 4 is of a greater intensity than the other secondary peaks.

An additional point to note from the RA/AgTFA treatment concerns other possible sources of PSD fragments. Returning to Figure 7, in D the selection window is set to 3759 ± 30 u. This selects an apparently barren region, according to the linear mode spectrum of Figure 7A, yet it does produce PSD peaks. Three decay peaks are observed that approximately coincide with peaks 1, 2, and 3 in Figure 7C, though they are offset from them slightly. Significant contribution to the largest peak in Figure 7D from $(PS_{n=34} + Ag)^+$ ions (*m/z* 3707) passing at the edge of the acceptance window is doubtful, especially since the peak is still observed when the window is centered at *m/z* 3769. The most probable explanation for the peaks in Figure 7D is the decay of some ion or ions for which the corresponding linear mode peaks are obscured by noise in Figure 7A.

Dithranol/AgTFA Treatment

The dithranol/AgTFA treatment is the one case for which loss of MaSalt from the $(PS + MaSalt + M)^+$ adduct does not produce an especially prominent reflectron mode secondary series, though a series can be attributed to it. There are indications of secondary series in the linear mode spectra for this treatment (Figure 10A), but none are well defined. There is stronger evidence of several secondary series in the reflectron

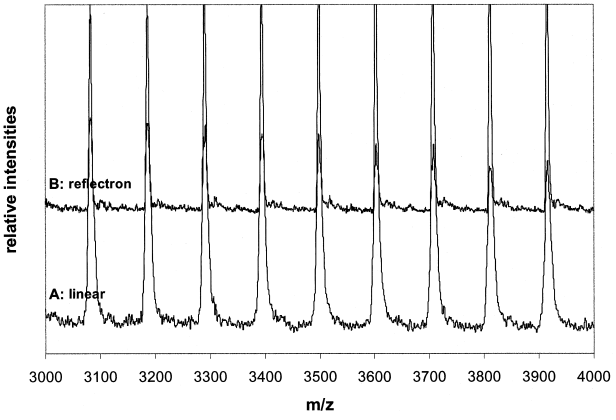

Figure 10. Partial (**A**) linear mode and (**B**) reflectron mode MALDI mass spectra of PS3900 obtained using the dithranol/AgTFA treatment. Though there are hints of secondary series in both spectra, none are well defined.

mode spectra (Figure 10B), although the secondary peaks are not very well defined there, either. Most prominent are a series at about +20 u with respect to the main series that is probably due to $(PS + MaSalt + Ag)^+$ and another series at about +60 u that has not yet been assigned. It should be pointed out that for all of the AgTFA treatments, the presence of a $(PS + 2Ag)^+$ adduct series cannot be verified, because its expected position is only +4 u from the $(PS + Ag)^+$ series.

In Figure 11A, the $(PS_{n=35} + Ag)^+$ ion is selected with a mass window of ±50 u. Three fragment peaks appear, and, consistent with the results of the other treatments, their mass assignments fit loss of styrene units. Note that other ions are included in the selection window, though their resolution remains poor. These are presumed to be adducts, and the most prominent appears to be $(PS_{n=32} + MaSalt + Ag)^+$, at +21 u with respect to the main peak. When the mass selection

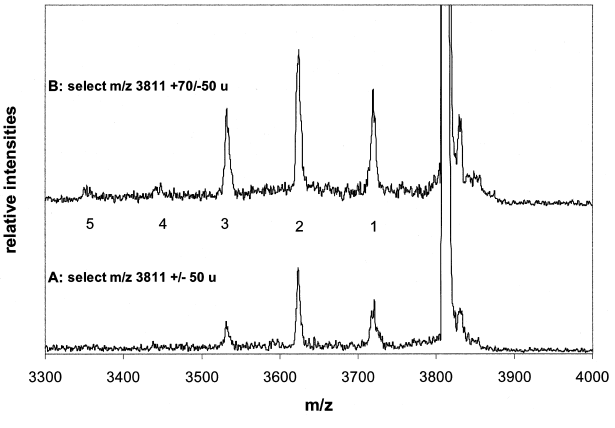

Figure 11. Partial PSD mode MALDI mass spectra of PS3900 obtained using the dithranol/AgTFA treatment. The spectra are calibrated for parent ions. In **A** the selection window is set to *m/z* 3811 ± 50 u, and fragment peaks are observed at positions 1, 2, and 3. In **B** the selection window is widened to +70 u/−50 u and additional fragment peaks are observed at positions 4 and 5. The relative intensities of peaks 1, 2, and 3 also change.

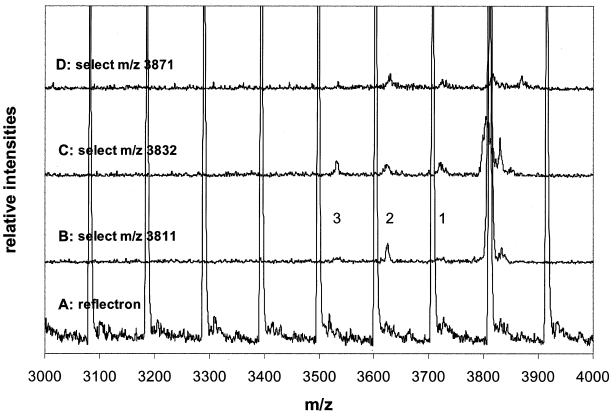

Figure 12. Partial (**A**) reflectron mode and (**B**, **C**, and **D**) PSD mode MALDI mass spectra of PS3900 obtained using the dithranol/AgTFA treatment. The PSD spectra are calibrated for parent ions. The mass selection window used for **B**, **C**, and **D** is ±30 u. In **B** the $(PS_{n=35} + Ag)^+$ ion at *m/z* 3811 is selected, and fragment peaks 1, 2, and 3 are observed. In **C** the window is moved to select the $(PS_{n=32} + MaSalt + Ag)^+$ ion at *m/z* 3832. The same three fragment peaks are observed, but at different relative intensities. In **D** an unidentified ion is selected with the window centered at *m/z* 3871. Fragment peaks are again observed at the same three positions, along with a peak that is consistent with a loss of 60 u from the selected ion.

window is widened to +70 u/−50 u (Figure 11B), there appear to be additional adducts included within the selection window. The first and third fragment peak intensities increase relative to that of the middle peak, and two additional peaks appear at lower mass. The additional decay products also appear to be of the form $(PS + Ag)^+$, so that they are likely to be due either directly to loss of adducted material or to decay which includes loss of styrene from PS oligomers.

In Figure 12 the mass selection window is narrowed to ±30 u. A normal reflectron mode spectrum is shown for comparison in Figure 12A. The $(PS_{n=35} + Ag)^+$ ion is again selected in Figure 12B, and again some adducts appear to be included in the selection window. Fragment peaks 1, 2, and 3, consistent with loss of styrene units from $(PS_{n=35} + Ag)^+$, are observed as before, with peak 2 much more prominent than the other two. In Figure 12C the $(PS_{n=32} + MaSalt + Ag)^+$ ion is selected. The $(PS_{n=35} + Ag)^+$ ion is partially included, as well as other probable adduct ions. The same three fragment peaks are observed, but here they are about equal in intensity. Peak 3 is consistent with a loss of MaSalt from the selected ion. Loss of a matrix molecule from $(PS_{n=32} + Ma + 2Ag)^+$ is not a good fit to peak 2, though it may contribute to broadening of the peak. Peak 1 requires a loss of about 125 u from $(PS_{n=32} + MaSalt + Ag)^+$, which does not seem to be a probable loss. In Figure 12D the ion at about +60 u with respect to the $(PS_{n=35} + Ag)^+$ ion is selected. Again, other adducts may also be included. The same three fragment ions appear, though peak 3 is very small. A peak that corresponds to a loss of about 60 u from the selected ion is also observed.

Several general points can be made from the foregoing examples. First, most of the PSD product ions are of the form $(PS + M)^+$, i.e., the product ions have formulas the same as main series ions. The only apparent exception is the peak assigned as loss of Ma from $(PS + Ma + 2Cu)^+$ in the Cu(II)TFA treatments. Thus loss of adducted material and elimination of styrene units appear to be the only decay processes. A related point is that two or more types of parent ions may decay to give the same product ion. Although $(PS + MaSalt + M)^+$ is in most cases the most prominent adduct ion observed, other adducts, mostly unidentified at this point, are apparently formed and decay. The suspected additional adducts are most easily observed with the dithranol/AgTFA treatment, but they appear to form to some extent with all the treatments. For some decay peaks there is a single decay process that clearly makes the dominant contribution, e.g., loss of MaSalt from $(PS + MaSalt + M)^+$, but for others there may not be a single dominant source.

For all treatments the number of secondary series that are actually formed is larger than is initially apparent from the linear and reflectron mode spectra. This is partially due to the relatively low intensity of most of the secondary series, but is also due to the multiplicity of peaks. For a given treatment each PS oligomer forms similar adduct and decay products, and, as a result, peak overlap contributes to the apparent noise level. As was demonstrated in several cases, some peaks become visible only when the ion selector is used, because that eliminates some of the sources of overlap. Some adduct peaks that are not distinct in the linear mode spectra may not be visible even when the ion selector is used, due to a high decay rate. That is a probable explanation for the case presented in Figure 7D, where an apparently barren selection window produces decay peaks.

Post-Source Decay of $(PS + M)^+$ Ions

It is apparent that at least in some cases decay peaks observed when $(PS + M)^+$ ions are selected are actually due to decay of other adducts included in the selection window. For all treatments, however, there remain decay peaks which are consistent with loss of styrene units from $(PS + M)^+$ and for which there are no obvious alternative explanations. Still, we cannot be wholly confident that such an assignment is correct. One reason for doubt is that there are treatment-to-treatment differences in the intensity patterns of these peaks, even after the effect of the loss of MaSalt from $(PS + MaSalt + M)^+$ is taken into account. For example, compare Figures 6B, 7C, and 11. Figures 11 and 12 strongly suggest that in the case of the dithranol/AgTFA treatment, decay of unidentified adducts contributes at least partially to the suspected loss-of-styrene peaks. It is possible that such decay accounts totally for these peaks. Likewise, when one considers that not all adduct peaks may be apparent in linear or reflectron mode spectra, the possibility exists that adduct decay at least contributes to the suspected loss-of-styrene peaks in the other five treatments.

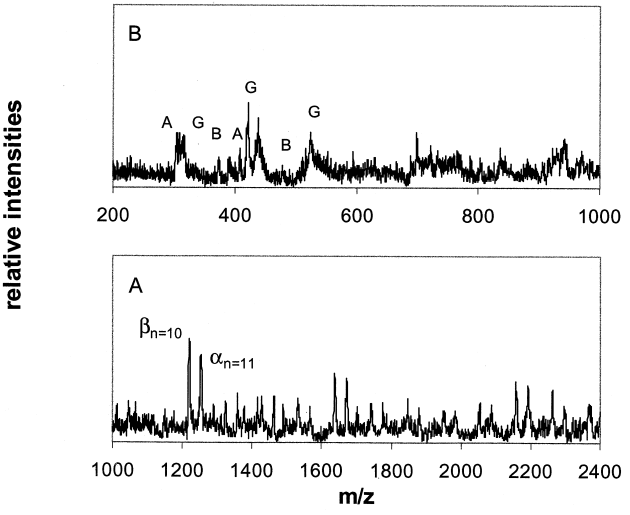

Figure 13. Portions of a PSD mode MALDI mass spectrum of PS3900 obtained using the IAA/AgTFA treatment. The $(PS_{n=35} + Ag)^+$ ion at *m/z* 3811 is selected with a mass window of ±60 u. The spectrum is calibrated to give the fragment ion masses. In **A** the region from *m/z* 1000 to 2400 is shown. Two series of peaks, α and β, are observed, with nominal masses given by $[(104)_n + Ag]$ and $[(104)_n + 70 + Ag]$, respectively. Only one peak from each series is marked, but the series extend at least from $n = 10$ to 20. In **B** the region from *m/z* 2000 to 1000 is shown. The marked peaks appear to match polystyrene fragment peaks described in [29].

At normally used laser intensities, no polystyrene decay is observed other than the aforementioned possible loss of from one to several styrene units. At higher laser intensities, peaks that are unambiguously due to PS decay are observed. These PSD fragments are similar for all six treatments and are of low intensity. Decay of the $(PS_{n=35} + M)^+$ ion was examined for all treatments, but similar results were observed for other oligomers. Figure 13 shows parts of a PSD spectrum for the IAA/AgTFA treatment. Two series of fragments are observed (Figure 13A) having approximately equal intensities, with nominal masses given by $[(104)_n + M]^+$ (α series) and $[(104)_n + 70 + M]^+$ (β series). The series are observed from roughly $n = 10$ to $n = 20$. Similar series for PS, though at noticeably higher signal-to-noise ratio, were observed in liquid secondary ion collision-induced dissociation (LSI-CID) mass spectra by Jackson et al. [19], in MALDI-CID mass spectra by Jackson et al. [29], and in field desorption mass-analyzed ion kinetic energy (FD-MIKE) spectra by Craig and Derrick [47]. Copper and silver cationized PS parent ions were produced in the LSI-CID [19] and MALDI-CID [29] work, and radical cation PS parents were produced in the FD-MIKE [47] work. The α and β series have been proposed to arise from rearrangements involving six-membered ring intermediates [19, 47]. In the FD-MIKE work [47], two other series of ions, called the A and the B series, in which the charge was retained on the fragments complimentary to the α and β frag-

ments, were also observed and were, in fact, at higher intensities than were the α and β series. The A and B series are not observed in the present work, nor were they observed in the LSI-CID [19] or MALDI-CID [29] work. Jackson et al. [19] suggested that, for cationized PS, greater electron delocalization at the fragment end may aid in stabilizing the α and β ions in comparison to the A and B ions.

Another group of peaks appear at *m/z* values lower than the α and β series (Figure 13B). These tend to be somewhat broad and without well-defined apexes, but several of them appear to fit with low mass series described by Jackson et al. (called the A, B, and G series in that work [29]. Additional peaks are found at estimated masses of (202 + M) and (282 + M), along with a few peaks found either in the AgTFA treatment PSD spectra or in the Cu(II)TFA treatment PSD spectra, but not in both. In order to observe these peaks, laser energy and detector gain were increased to levels well past those we normally use to acquire MALDI mass spectra of PS.

The higher mass decay peaks tentatively assigned as due to loss of styrene units have no counterpart in the works cited above. They have the same formula, apart from the metal cation, as the A series peaks described by Craig and Derrick [47] but are not likely to be formed by the same mechanism. As noted above, the α and β series ions are complimentary to the A and B series ions. The possible loss-of-styrene ions appear to form at lower energy than is required for formation of the α and β series ions. We would also expect to see the related B ions if the mechanism that produces A ions was operable [47].

Loss of styrene from $(PS + M)^+$ perhaps could occur through a free-radical mechanism such as β-scission or back-biting [48]. In these cases, however, we would expect to see a broader distribution of styrene losses than is observed. At present we are not able to answer definitively the question of whether $(PS + M)^+$ is decaying by loss of styrene units. Because we have not yet identified specific adduct decay processes to account for all the peaks that appear to be due to loss of styrene, however, it must be considered a possibility.

Analytical Implications

The presence of adduct and decay peaks creates confusion about what species are truly present in a polymer sample. These peaks can be identified as such, as was done here, by using more than one treatment and by PSD experiments. However, if no testing for them is done, such peaks may be misinterpreted; the presence of extra sets of end groups or other sample heterogeneities may be concluded when it is not warranted. The converse problem is also possible, i.e., minor species actually present in a polymer sample may be more difficult to detect due to overlap and an effective rise in the noise level. It is doubtful that PS is unique in its tendency to form adducts, so that similar difficulties may hold for MALDI analysis of other classes of polymers.

The effect of adduct and decay peaks on molecular mass determinations of synthetic polymers or other samples which possess a distribution of mass must also be considered. The ion intensity distributions appear to follow from the main series ion intensity distribution, with an appropriate shift due to the adducted species or to PSD. The largest of the adduct and decay peaks usually are on the order of 5% to 10% of the intensity of the main series ions, though on occasion we have obtained spectra in which they have a considerably larger relative intensity. Assuming typical relative intensities, the linear mode RA/AgTFA treatment is subject to the largest error in molecular mass determinations. In this case the $(PS + MaSalt + Ag)^+$ ion appears at a shift of about four repeat units (+408 u) from the peak position of the main series ion with the same number of repeat units. Any other adducts also necessarily appear at higher masses than the corresponding main series ions. An estimate of the error in M_N due to adduct offset, assuming that moments are determined by summing continuously over the distribution, is obtained by adding 5% to 10% of 408 u to the correct M_N value. Thus the error in M_N in this case should be +20 to +40 u. It should be no larger for the other treatments. The corresponding errors in M_W should be only slightly larger. As long as the adduct peak intensities follow from the main series peak intensities, these errors should not change much even for more polydisperse samples. In reflectron mode the errors should be smaller, because the $(PS + MaSalt + M)^+$ adduct intensity is reduced by decay, and the resulting positions of the products more closely match the corresponding positions of the $(PS + M)^+$ ions with the same number of repeat units. Any contribution from decay of $(PS + M)^+$ ions would tend to counter the positive offset of adduct peaks. This analysis assumes that adducts and their decay products appear at relatively well-defined peak positions. To the extent that poorly resolved decay products contribute to baseline irregularities, such as sloped baselines or humps under the polymer distribution, they can potentially have a more serious effect on polymer molecular mass determinations.

Conclusions

Secondary series that appear in the MALDI-TOF mass spectra of polystyrene are largely due to adduct formation and decay. Adduct formation and associated decay is more extensive than is apparent from the linear or reflectron mode mass spectra, as some peaks are hidden due to the multiplicity of secondary series. Some hidden peaks can be revealed by PSD analysis, because isolation of a mass window largely excludes interfering decay peaks.

Series due to adduct formation and decay are most obviously a problem for qualitative analysis. They contribute to a loss of resolution and may obscure signal

from minor species in a sample. They may also lead to a false positive identification of minor species. The secondary series discussed in this work are not a source of serious error for molecular mass determinations; however, adduct formation and decay are potentially a source of baseline irregularities, and that may have more significant consequences for quantitative analysis. In this work we examined only MALDI analysis of PS. It is not unreasonable to suppose that similar adduct formation and decay occurs for other types of polymers.

The secondary series also complicate PSD analysis. With few exceptions, it appears that decay under normally used conditions is due to either loss of adducted species to form $(PS + M)^+$ ions or loss of styrene units from $(PS + M)^+$ ions. We were unable to determine conclusively whether the latter decay actually occurs, however, or whether all observed decay was adduct decay. At higher laser fluences than normally used, PSD of $(PS + M)^+$ ions definitely does occur. The fragment ions so produced are of lower masses than the decay peaks observed under normal conditions, and the peaks due to these ions are of low intensity.

The question of how the observed adduct species are formed remains to be answered. In a broad sense the answer is either that they are performed or that they form due to interactions during or after desorption, or some combination of these. If it is assumed that PS oligomers are isolated in the matrix, then it may be reasonably suspected that in some cases some of the surrounding matrix molecules will remain attached to them upon desorption. Molecular dynamics simulations of laser desorption and ablation of organic solids, although not addressing matrix-analyte adduct formation directly, indicate that direct ejection of molecular clusters of various sizes does occur [49, 50]. In a mass spectrum, however, one observes only species that have been ionized. All ejected species may not be represented in this subset. There is considerable evidence that ionization in MALDI can occur through selvedge or gas phase reactions [44, 51]. There is also evidence that combination of species that are not adjacent in the condensed phase can occur in MALDI [52], and, at least in some cases, in other desorption/ionization methods [53, 54]. Thus the combination of matrix species and PS oligomers subsequent to the laser pulse should also be suspected as a possibility.

References

1. Bahr, U.; Deppe, A.; Karas, M.; Hillenkamp, F. *Anal. Chem.* **1992,** *64*, 2866–2869.
2. Danis, P. O.; Karr, D. E.; Mayer, F.; Holle, A.; Watson, C. H. *Org. Mass Spectrom.* **1992,** *27*, 843–846.
3. Burger, H. M.; Muller, H. M.; Seebach, D.; Bornsen, K. O.; Schar, M.; Widmer, H. M. *Macromolecules* **1993,** *26*, 4783–4790.
4. Scrivens, J. H. *Adv. Mass Spectrom.* **1995,** *13*, 447.
5. Montaudo, G. *Trends Polym. Sci.* **1996,** *4*, 81–86.
6. Tang, X.; Dreifuss, P. A.; Vertes, A. *Rapid Commun. Mass Spectrom.* **1995,** *9*, 1141–1147.
7. Jackson, C.; Larsen, B.; McEwen, C. *Anal. Chem.* **1996,** *68*, 1303–1308.
8. Axelsson, J.; Scrivener, E.; Haddleton, D. M.; Derrick, P. J. *Macromolecules* **1996,** *29*, 8875–8882.
9. Martin, K.; Spickermann, J.; Rader, H. J.; Mullen, K. *Rapid Commun. Mass Spectrom.* **1996,** *10*, 1471.
10. Schriemer, D. C.; Li, L. *Anal. Chem.* **1997,** *69*, 4169–4175.
11. Schriemer, D. C.; Li, L. *Anal. Chem.* **1997,** *69*, 4176–4183.
12. Danis, P. O.; Karr, D. E.; Simonsick, W. J.; Jr; Wu, D. T. *Macromolecules* **1995,** *28*, 1229–1232.
13. Danis, P. O.; Karr, D. E.; Xiong, Y.; Owens, K. G. *Rapid Commun. Mass Spectrom.* **1996,** *10*, 862–868.
14. Montaudo, G.; Montaudo, M. S.; Puglisi, C.; Samperi, F. *Rapid Commun. Mass Spectrom.* **1995,** *9*, 453–460.
15. Garozzo, D.; Impallomeni, G.; Spina, E.; Sturiale, L.; Zanetti, F. *Rapid Commun. Mass Spectrom.* **1995,** *9*, 937–941.
16. Wallace, W. E.; Guttman, C. M.; Blair, W. R. *Proceedings of the 45th ASMS Conference on Mass Spectrometry*; Palm Springs, CA, June 1–5, 1997; p 1273.
17. Weidner, S.; Kuhn, G.; Just, U. *Rapid Commun. Mass Spectrom.* **1995,** *9*, 697–702.
18. van Rooij, G. J.; Duursma; M. C.; Heeren, R. M. A.; Boon, J. J.; de Koster, C. G. *J. Am. Soc. Mass Spectrom.* **1996,** *7*, 449–457.
19. Jackson, A. T.; Jennings, K. R.; Scrivens, J. H. *J. Am. Soc. Mass Spectrom.* **1997,** *8*, 76–85.
20. Montaudo, G.; Garozza, D.; Montaudo, M. S.; Puglisi, C.; Samperi, F. *Macromolecules* **1995,** *28*, 7983–7989.
21. Wilczek-Vera, G.; Danis, P. O.; Eisenberg, A. *Macromolecules* **1996,** *29*, 4036–4044.
22. Schriemer, D. C.; Whittal, R. M.; Li, L. *Macromolecules* **1997,** *30*, 1955–1963.
23. Wilczek-Vera, G.; Yu, Y.; Waddell, K.; Danis, P. O.; Eisenberg, A. *Macromolecules* **1999,** *32*, 2180–2187.
24. Yalcin, T.; Schriemer, D. C.; Li, L. *J. Am. Soc. Mass Spectrom.* **1997,** *8*, 1220–1229.
25. Lattimer, R. P. *J. Am. Soc. Mass Spectrom.* **1992,** *3*, 225–234.
26. Lattimer, R. P. *J. Am. Soc. Mass Spectrom.* **1994,** *5*, 1072–1080.
27. Selby, T. L.; Wesdemiotis, C.; Lattimer, R. P. *J. Am. Soc. Mass Spectrom.* **1994,** *5*, 1081–1092.
28. Scrivens, J. H.; Jackson, A. T.; Yates, H. T.; Green, M. R.; Critchley, G.; Brown, J.; Bateman, R. H.; Bowers, M. T.; Gidden, J. *Int. J Mass Spectrom. Ion Processes* **1997,** *165/166*, 363–375.
29. Jackson, A. T.; Yates, H. T.; Scrivens, J. H.; Green, M. R.; Bateman, R. H. *J. Am. Soc. Mass Spectrom.* **1998,** *9*, 269–274.
30. Gidden, J.; Jackson, A. T.; Scrivens, J. H.; Bowers, M. T. *Int. J. Mass Spectrom. Ion Processes* **1999,** *188*, 121–130.
31. Pastor, S. L.; Wilkins, C. L. *Int. J. Mass Spectrom. Ion Processes* **1998,** *175*, 81–92.
32. Spengler, B.; Kirsch, D.; Kaufmann, R. *Rapid Commun. Mass Spectrom.* **1991,** *5*, 198–202.
33. Spengler, B.; Kirsch, D.; Kaufmann, R. *J. Phys. Chem.* **1992,** *96*, 9678–9684.
34. Spengler, B.; Kirsch, D.; Kaufmann, R.; Jaeger, E. *Rapid Commun. Mass Spectrom.* **1992,** *6*, 105–108.
35. Kaufmann, R.; Spengler, B.; Lutzenkirchen, F. *Rapid Commun. Mass Spectrom.* **1993,** *7*, 902–910.
36. Kaufmann, R.; Kirsch, D.; Spengler, B. *Int. J. Mass Spectrom. Ion Processes* **1994,** *131*, 355–385.
37. Kaufmann, R.; Chaurand, P.; Kirsch, D.; Spengler, B. *Rapid Commun. Mass Spectrom.* **1996,** *10*, 1199–1208.
38. Spengler, B. *J. Mass Spectrom.* **1997,** *32*, 1019–1036.
39. Karas, M.; Bahr, U.; Strupat, K.; Hillenkamp, F.; Tsarbopoulos, A.; Pramanik, B. N. *Anal. Chem.* **1995,** *67*, 675–679.
40. Brown, R. S.; Lennon, J. J. *Anal. Chem.* **1995,** *67*, 1998–2003.
41. Brown, R. S.; Lennon, J. J. *Anal. Chem.* **1995,** *67*, 3990–3999.

42. Brown, R. S.; Carr, B. L.; Lennon, J. J. *J. Am. Soc. Mass Spectrom.* **1996,** *7*, 225–232.
43. Cotter, R. J. *Time-of-Flight Mass Spectrometry*; American Chemical Society: Washington, DC, 1997.
44. Knochenmuss, R.; Lehmann, E.; Zenobi, R. *Eur. Mass Spectrom.* **1998,** *4*, 421–427.
45. Blair, W. R.; Fanconi, B. M.; Goldschmidt, R. J.; Guttman, C. M.; Wallace, W. E.; Wetzel, S. J.; VanderHart, D. L. *Proceedings of the 47th ASMS Conference on Mass Spectrometry*; Dallas, TX, June 13–17, 1999; p 913.
46. Certain commercial equipment is identified in this article in order to adequately specify the experimental procedure. In no case does such identification imply recommendation or endorsement by the National Institute of Standards and Technology, nor does it imply that the items identified are necessarily the best available for the purpose.
47. Craig, A. G.; Derrick, P. J. *Aust. J. Chem.* **1986,** *39*, 1421–1434.
48. Guyot, A. *Polym. Degr. Stab.* **1986,** *15,* 219–235.
49. Zhigilei, L. V.; Kodali, P. B. S.; Garrison, B. J. *Chem. Phys. Lett.* **1997,** *276*, 269–273.
50. Zhigilei, L. V.; Garrison, B. J. *Appl. Phys. Lett.* **1999,** *74*, 1341–1343.
51. Zenobi, R.; Knochenmuss, R. *Mass Spectrom. Rev.* **1998,** *17*, 337–366.
52. Rashidezadeh, H.; Guo, B. *J. Am. Soc. Mass Spectrom.* **1998,** *9*, 724–730.
53. Pachuta, S. J.; Cooks, R. G. *Chem. Rev.* **1987,** *87*, 647–669.
54. Sunner, J. *Org. Mass Spectrom.* **1993,** *28*, 805–823.